International Journal of Computational Intelligence and Informatics, Vol. 1 : No. 4, January - March 2012

Mammogram Image Segmentation using Rough Set Theory

Thangavel. K
Department of Computer Science,
Periyar University,
Salem - 636 011, Tamil Nadu, India.
drktvelu@yahoo.com

Velayutham. C
Department of Computer Science,
Periyar University,
Salem- 636 011, Tamil Nadu, India
cvelayutham22@yahoo.com

Abstract

The presence of microcalcification in mammogram image has been considered as a indicator of malignant types of breast cancer, and its detection is important to prevent and treat the disease. This paper proposes an effective approach, relative dependency measure using the Rough Set Theory (RST) in order to automatic detection of microcalcification in digitized mammogram images. The preprocessing of mammogram image is essential before detection and segmentation of microcalcification. However, the presence of artifacts and pectoral muscle can disturb the detection of microcalcification and reduce the rate of accuracy in the Computer Aided Diagnosis (CAD). Its inclusion can affect the results of intensity-based image processing methods and needs to be identified and removed before further analysis. These processes are performed in the preprocessing stage. 117 mammogram images from the MIAS database have been used for evaluation. The computational results are evaluated with the reports already available in the MIAS database.

Keywords: Microcalcification detection, Segmentation, Mammography, Computer-Aided Diagnosis, Rough Set Theory

1. Introduction

Breast cancer is one of the most dangerous types of cancer among women around the world. Currently, the most effective method for early detection of breast cancer is mammography. Microcalcifications (MCs) are tiny deposits of calcium in breast tissue, which appear in a mammogram as small clusters of a few pixels, with relatively high intensity and closed contours compared with neighboring pixels. MC clusters are primary signs of breast cancer, where early detection is important to prevent and treat the disease. However, achieving detection of all MCs is not an easy task, since there is a poor contrast between MCs and their surrounding tissues [1]. Breast cancer is a leading cause of cancer deaths among women. For women in US and other developed countries, it is the most frequently diagnosed cancer. About 2100 new cases of breast cancer and 800 deaths are registered each year in Norway [2]. In India, a death rate of one in eight women has been reported due to breast cancer[1].

All the CAD systems require, as a first stage, the segmentation of each mammogram into its representative anatomical regions, i.e., the breast border, the pectoral muscle and the nipple, as in the work by Ferrari et al. [3]. The breast border extraction is a necessary and cumbersome step for typical CAD systems, as it must identify the breast region independently of the digitization system, the orientation of the breast in the image and the presence of noise, including imaging artifacts. The goal is to exclude the background from the subsequent processing steps, reducing the image file size without losing anatomic information. It should also have a fast running time and be sufficiently precise, in order to improve the accuracy of the overall CAD system.

There are a large number of different types of mammographic abnormality. In the majority of cases, however, the abnormalities are either micro-calcifications or masses. Micro-calcifications usually form clusters and individual micro-calcifications can range from 20 to several hundred microns in diameter. On the other hand, a breast mass is a generic term to indicate a localised swelling, protuberance, or lump in the breast. Masses can be caused by different processes: from natural changes in the breast to cancerous processes. Masses are characterised by their location, size, shape, margin, and associated findings (i.e. architectural distortion, contrast). Fig. 1 shows different masses according to their shape and margin (the border of the mass). These associated properties are examined by radiologists as they are strongly correlated with the classification (benign versus malignant) of the mass. It is generally accepted that mass detection is a more challenging problem than the detection of micro-calcifications, not only for the large variation in size and shape in which masses can appear in a mammogram but also because masses often exhibit poor image contrast(Oliver et al.(2010))[4].

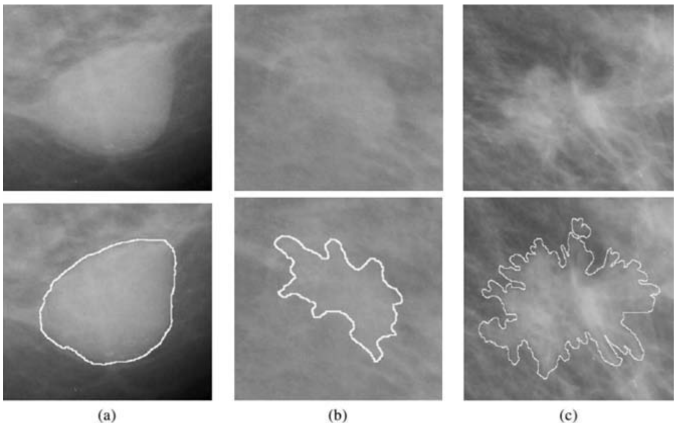

Fig. 1.Three types of mass with different shape and margin: (a) circular shapeand circumscribed margin, (b) lobular shape and well defined margin, and (c)spiculated shape and ill-defined margin

Already much work has been carried out in this area. Oliver et al.(2010)[4] have reviewed some of the approaches of automatic detection and segmentation of masses in mammographic images, highlighting the key-points and main differences between the used strategies. Dubey et al., (2010)[5] have compared two different semi-automated methods, viz., level set and marker controlled watershed methods which performed segmentation of tumor. Domınguez et al,(2008)[6] have presented a method for automatic detection of mammographic masses. The regions were segmented via thresholding at multiple levels, and a set of features were computed from each of the segmented regions. A region-ranking system was also presented that identifies the regions most likely to represent abnormalities based on the features computed. The method was tested on 57 mammographic images of masses from the Mini-MIAS database, and achieved a sensitivity of 80%. Wu et al.,(2008)[7] have proposed top-down region dividing based approach for image segmentation, which combines the advantages of both histogram-based and region-based approaches. Thangavel et al.[8], have used Ant colony optimization technique to segment the microcalcification region. In this paper, a novel Rough Set Theory based approach is proposed for segmentation of region of interest and compared with manual segmentation suggested in the MIAS database.

The rest of the paper is organized as follows: Section 2 presents an introduction to the Rough Set Theory. Section 3 presents the feature extraction methods. Section 4 describes the proposed method for detection of pectoral muscle using RST. The experimental results are discussed in section 5 and conclusion is presented in section 6.

2. Rough Set Theory – An Overview

Rough Set Theory (RST) is used as a tool to discover data dependencies and to reduce the number of attributes contained in a dataset using the data alone, requiring no additional information [9][10] [11]. Over the past ten years, RST has become a topic of great interest among researchers and has been applied to many domains. Given a dataset with discretized attribute values, it is possible to find a subset (termed a reduct) of the original attributes using RST that are the most informative; all other attributes can be removed from the dataset with minimal information loss.

It possesses many features in common (to a certain extent) with the Dempster-Shafer theory of evidence, and fuzzy set theory [12]. The rough set itself is the approximation of a vague concept (set) by a pair of precise concepts called lower and upper approximations. These are the classification of the domain of interest into disjoint categories. The lower approximation is a description of the domain objects which are known with certainty to belong to the subset of interest,where as the upper approximation is a description of the objects which possibly belong to the subset. The approximations are constructed with regard to a particular subset of features.

It works by making use of the granularity structure of the data only. This is a major difference when compared with Dempster-Shafer theory and fuzzy set theory which require probability assignments and membership values respectively. However, this does not mean that no model assumptions are made. In fact by using only the given information, the theory assumes that the data is true and accurate reflection of the real world (which may not be the case). The numerical and other contextual aspects of the data are ignored which may seem to be a significant omission, but keeps model assumptions to a minimum.

Basic Concepts

Let $I = (U, A \cup \{d\})$ be an information system, where U is the universe with a non-empty set of finite objects. A is a non-empty finite set of conditional attributes, and d is the decision attribute (such a table is also called decision table), $\forall a \in A$ there is a corresponding function $f_a : U \to V_a$, where V_a is the set of values of a. If $P \subseteq A$, there is an associated equivalence relation:

$$\mathrm{IND}(P) = \{(x, y) \in U \times U \mid \forall a \in P,\ f_a(x) = f_a(y)\} \tag{1}$$

The partition of U generated by IND(P) is denoted by U/P. If $(x, y) \in \mathrm{IND}(P)$, then x and y are indiscernible by attributes from P. The equivalence classes of the P-indiscernibility relations are denoted by $[x]_P$. Let $X \subseteq U$, the P-lower approximation $\underline{P}X$ and P-upper approximation $\overline{P}X$ of set X can be defined as:

$$\underline{P}X = \{x \in U \mid [x]_P \subseteq X\} \tag{2}$$

$$\overline{P}X = \{x \in U \mid [x]_P \cap X \neq \phi\} \tag{3}$$

Let $P, Q \subseteq A$ be equivalence relations over U, then the positive, negative and boundary regions can be defined as:

$$\mathrm{POS}_P(Q) = \bigcup_{X \in U/Q} \underline{P}X \tag{4}$$

$$\mathrm{NEG}_P(Q) = U - \bigcup_{X \in U/Q} \overline{P}X \tag{5}$$

$$\mathrm{BND}_P(Q) = \bigcup_{X \in U/Q} \overline{P}X - \bigcup_{X \in U/Q} \underline{P}X \tag{6}$$

The positive region of the partition *U/Q* with respect to *P*, $\mathrm{POS}_P(Q)$, is the set of all objects of *U* that can be certainly classified to blocks of the partition *U/Q* by means of *P*. *Q* depends on *P* in a degree k ($0 \le k \le 1$) denoted by $P \Rightarrow_k Q$

$$k = \gamma_P(Q) = \frac{|\mathrm{POS}_P(Q)|}{|U|} \tag{7}$$

where*P* is a set of conditional attributes and *Q* is the decision, $\gamma_P(Q)$ is the quality of classification (Pawlak et al.,1997)[10]. If $k = 1$, *Q* depends totally on *P*, if $0 < k < 1$, *Q* depends partially on *P*, and if $k = 0$ then *Q* does not depend on *P*. The goal of attribute reduction is to remove redundant attributes so that the reduced set provides the same quality of classification as the original. The set of all reducts is defined as:

$$\mathrm{Red} = \{R \subseteq C \mid \gamma_R(D) = \gamma_C(D), \forall B \subset R, \gamma_B(D) \neq \gamma_C(D)\} \tag{8}$$

A dataset may have many attribute reducts. The set of all optimal reducts is:

$$\mathrm{Red}_{\min} = \{R \in \mathrm{Red} \mid \forall R' \in \mathrm{Red}, |R| \le |R'|\} \tag{9}$$

3. Image Pre-Processing

3.1 Gray level Normalization of image

The distribution of gray levels of mammogram images may vary greatly; however, the ranges of the intensities are narrow. Normalization is a necessary step, and we normalize the mammogram image by mapping the intensity levels into the range [$Ng_{\min}$, $Ng_{\max}$]:

$$g(i,j) = \frac{(g(i,j) - g_{\min})(Ng_{\max} - Ng_{\min})}{(g_{\max} - g_{\min})} \tag{10}$$

where $g(i,j)$ is a gray level value at the coordinate (*i*, *j*), $g_{\min}$, $g_{\max}$ are the minimum and maximum intensity levels of the original image; $Ng_{\min}$, $Ng_{\max}$ are the minimum and maximum intensity levels of the normalized image respectively.

3.2 Elimination of Artifacts

The black parts of the image as well as the existing artifacts such as written labels etc., are removed using cropping operations. An example of cropping that eliminates the artifacts and the black background is depicted in Fig. 2. The cropping operation is used to eliminate noise before the image enhancement. The cropping operation is done automatically by sweeping through the image and cutting horizontally and vertically the image those parts, that had the mean less than a certain threshold. Fig. 2(a) shows the original image. The image enhancement process such as removal of labels and artifact are applied and the corresponding images are shown in Fig. 2(b). Fig. 2(c) shows transformed image.

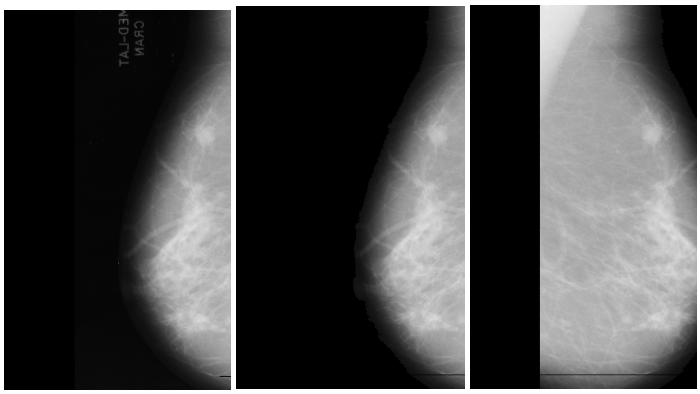

(a) (b) (c)

Fig. 2. Example of Image pre-processing for the image (mdb023.pgm), (a) original image, (b) After removing artifacts, (c) Transformed image.

4. Feature Extraction

The texture analysis matrix itself does not directly provide a single feature that may be used for texture discrimination. Instead, the matrix can be used as a representation scheme for the texture image and the features are computed.

4.1 Gray Level Co-occurrence Matrix (*GLCM*)

Generally, the problem of texture discrimination based on statistical approach consists of the analysis of a set of co-occurrence matrices [13], [14]. In this matrix, the indices of rows and columns represent the given range of the image gray levels, and the value *P*(*i*, *j*) stored in the position (*i*, *j*) is the frequency that gray levels *i* and *j* occur at distance = 1 and in the directions 0°, 45° ,90° , and 135°.

4.2 The Haralick Features

The features based on the distribution matrices should therefore capture some characteristics of textures such as homogeneity, coarseness, periodicity and others. Gulsrud et al.[15] Haralick et al. [13] have suggested 14 texture features, such as : angular second moment(f_1) , contrast(f_2), correlation(f_3), sum of squares: variance(f_4), inverse difference moment(f_5), sum average(f_6), sum variance(f_7), sum entropy(f_8), entropy(f_9), difference variance(f_{10}), difference entropy(f_{11}), information measures of correlation-I(f_{12}), information measures of correlation-II(f_{13}), the maximal correlation coefficient(f_{14}).

5. Proposed Method

5.1 Mammogram Image Segmentation

The image segmentation is a major step in image processing. Segmentation divides image into its constituent regions or objects. The level to which segmentation is carried out depends upon the problem being solved i.e., segmentation should stop when the 'Regions Of Interest' (ROI) in an application has been isolated. The presence of microcalcification in mammogram image has been considered as a indicator of malignant types of breast cancer, and its detection is important to prevent and treat the disease. This paper proposes an effective approach, relative dependency measure using the Rough Set Theory (RST) in order to automatic detect and segment microcalcification in digitized mammogram images. The segmentation of microcalcification is identified using an automatic thresholding method. The segmentation of microcalcification results are evaluated in terms radiologist identified information given in the MIAS database.

5.2 Relative dependency measure using RST

The selection of gray value (object) using Rough Set based unsupervised relative dependency measure Velayutham et al. [16]-[20].

$$\kappa_R(\{a\}) = \frac{|U/\mathrm{IND}(R)|}{|U/\mathrm{IND}(R\cup\{a\})|}, \forall a \in A \quad (11)$$

where a is an object which is used to evaluate the relative dependency and R contains all other objects. The relative dependency of each object is computed using equation (11). If relative dependency value of an object is equal to 1 then the object a is removed from R. If relative dependency value of an object a is not equal to 1 then the object a is a selected object and the corresponding gray value is used for segmentation. The proposed algorithm to identify the microcalcification and segmentation using RST is given in Fig. 4.

$I \leftarrow$ Read Pre-processed mammogram image
$I \leftarrow$ if the image I is right side transformed into left
$I_m \leftarrow$ Median Filter of I with window size [9, 9]
$th \leftarrow$ Peak threshold value from histogram (above the gray value 100)
    For each pixel from threshold value th
        $i \leftarrow i+1$
        $I_g \leftarrow I_m$
        $idx \leftarrow$ find($I_m \neq th_i$)
        $I_g(idx) \leftarrow 0$
        $G_i \leftarrow$ Construct GLCM using the image I_g with distance 1 and direction 0°
        For each j {j = 1, 2, …, 14} (14 Haralick features)
            $f_{ij} \leftarrow$ Compute feature using G_i
        end
    end
$N_{ij} \leftarrow$ Normalize the features f_{ij}
$D_{ij} \leftarrow$ Discretize N_{ij} using round of to desired integer
// threshold value selection using RST
$R \leftarrow D_{ij}$
    For each $R_i \in D_{ij}$
        If $\kappa_{R-\{D_i\}}(D_i) \neq 1$
            $Tr \leftarrow th + (i - 1)$
            break
        Else
            $R \leftarrow R - D_i$
        End
    End
// segmentation based on threshold value selected by RST
    $Y \leftarrow I_m$
    $idx \leftarrow$ find(I_m<tr)
    $Y(idx) \leftarrow 0$
Y is the microcalcification region.

Fig. 4. Segmentation Algorithm

5.3 Worked Example

In this section, the mammogram image, identification number *mdb023* from the MIAS database is considered. This mammogram image is malignant, fatty-glandular image and it contains well-defined or circumscribed masses. It is a right side breast image. For the automatic detection of microcalcification the right side image is transformed into the left side.

5.3.1 Median Filter

The median filtering is applied to remove the high frequency components in the mammogram image. The merit of using median filter is, it can remove the noise without disturbing the edges. For each pixel an 9×9 window of neighborhood pixels are extracted, and the median value is calculated for that window. The intensity value of the center pixel value is replaced with the median value. This procedure is done for all the pixels in the image to smoothen the mammogram image and the filtered image using median filter is shown in Fig. 5(b).

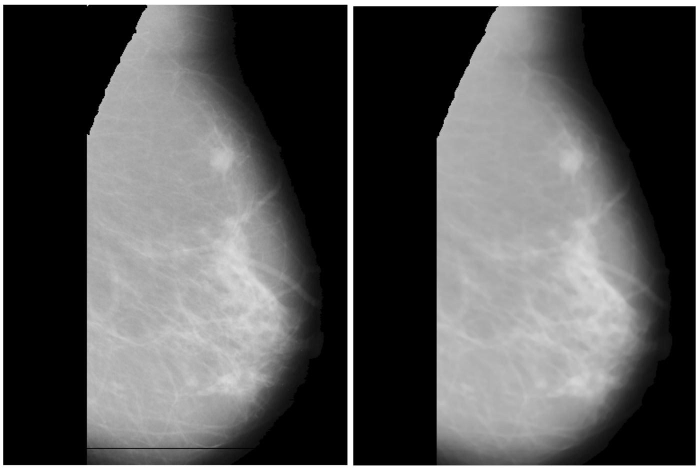

(a) (b)

Fig. 5 Image (mdb023) (a) Pectoral muscle suppressed image (b) Filter Image.

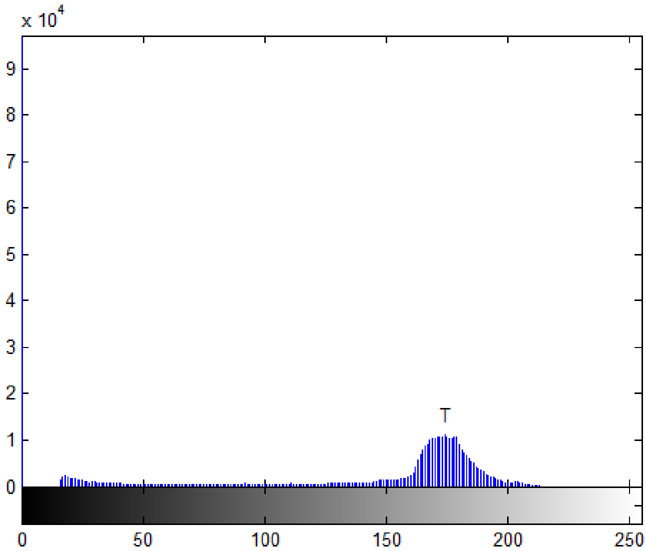

Fig. 6 Histogram of filtered image

The intensity and the contrast of the image are not same for all the images and it varies from image to image. Hence, the threshold value T is evaluated for every image using image histogram. Fig. 6 shows the histogram of the image Fig. 5(b).

According to the histogram threshold value T, only the corresponding gray value image is extracted from the enhanced image. The GLCM is computed from the image and the statistical feature is computed by using GLCM. Also, the features are created for the subsequent gray value image. Fig. 7 represents the images (a) to (c) for the gray values from 217 to 219 respectively. Table 1 represents the Haralick Statistical features for the gray valued images. Table 2 and Table 3 represents the normalized and discretised features respectively.

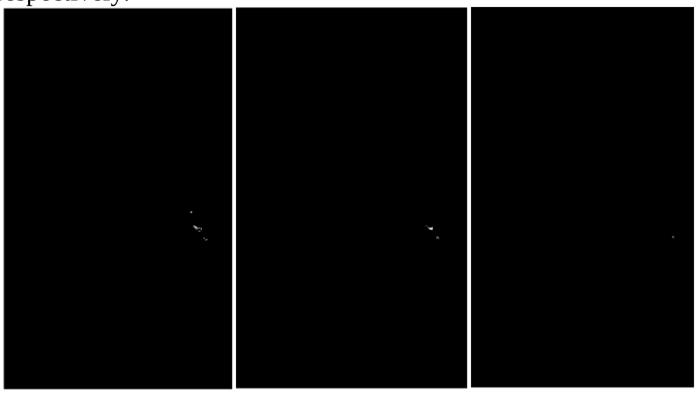

(a) (b) (c)

Fig. 7 Single gray valued images for the gray values (a) 217 (b) 218 (c) 219

Table 1 Haralick features extracted from the image using GLCM

	f_1	f_2	f_3	f_4	f_5	f_6	f_7	f_8	f_9	f_{10}	f_{11}	f_{12}	f_{13}	f_{14}
a	0.4998	0.9857	0.6129	0.8359	0.0152	0.5000	0.9906	0.0015	0.0015	0.0000	0.0015	-0.9999	0.0428	0.3495
b	0.4999	0.9856	0.6402	0.8198	0.0152	0.5000	0.9906	0.0010	0.0010	0.0000	0.0010	-1.0000	0.0324	0.3610
c	0.5000	0.9847	0.9458	0.3147	0.0152	0.5000	0.9901	0.0002	0.0002	0.0000	0.0002	-1.0000	0.0139	0.2047

Table 2 Normalized features

	f_1	f_2	f_3	f_4	f_5	f_6	f_7	f_8	f_9	f_{10}	f_{11}	f_{12}	f_{13}	f_{14}
a	0.5773	0.5776	0.4729	0.6895	0.5774	0.5774	0.5774	0.8256	0.8256	0.5825	0.8256	-0.5773	0.7721	0.6442
b	0.5773	0.5775	0.4939	0.6762	0.5773	0.5774	0.5774	0.5579	0.5579	0.5773	0.5579	-0.5773	0.5843	0.6654
c	0.5774	0.5770	0.7297	0.2596	0.5773	0.5774	0.5772	0.0842	0.0842	0.5723	0.0842	-0.5774	0.2499	0.3772

Table 3 Discretized features

	f_1	f_2	f_3	f_4	f_5	f_6	f_7	f_8	f_9	f_{10}	f_{11}	f_{12}	f_{13}	f_{14}
a	6	6	5	7	6	6	6	8	8	6	8	-6	8	6
b	6	6	5	7	6	6	6	6	6	6	6	-6	6	7
c	6	6	7	3	6	6	6	1	1	6	1	-6	2	4

Table 3 represents adescretized data set. Each row is considered as an object and it corresponds to a gray value. The object selection is carried out by the relative dependency measures using rough set theory. The selected object is considered as the boundary point for the segmentation. The input image for segmentation is shown in Fig. 8(a). The segmented output image is shown in Fig. 8(b).

An example of image segmentation process is given in Fig. 8.

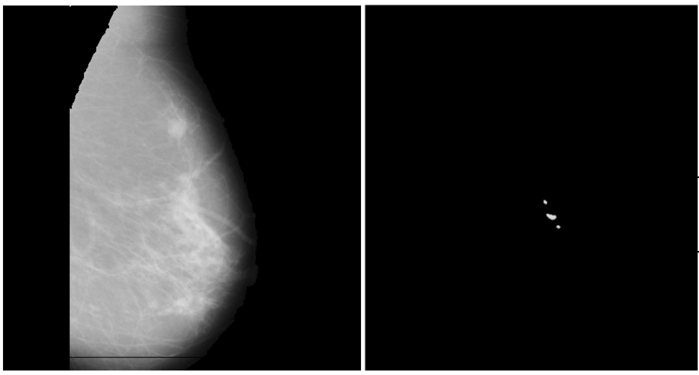

(a) (b)

Fig. 8. Example of Image segmentation (mdb023.pgm), (a) Image after removing artifacts and pectoral muscle, (b) Segmentation of microcalcification.

6. Experimental Results

The images used for the experimental analysis are taken from the Mammographic Image Analysis Society (MIAS) http://www.wiau.man.ac.uk/services/MIAS/MIASweb.html.[21]. It consists of 322 images, which belong to three big categories: normal, benign and malign. There are 208 normal images. 63 benign and 51 malign images are considered abnormal. In addition, the abnormal cases are further divided into six categories: microcalcification, circumscribed masses, spiculated masses, ill-defined masses, architectural distortion and asymmetry. All the images also include the locations of any abnormalities that may be present. The existing images consists of the location of the abnormality (like the centre of a circle surrounding the tumour), its radius, breast position (left or right), type of breast tissues (fatty, fatty-glandular and dense) and tumour type whether it is benign or malign. All the mammograms have medio-lateral oblique view. The calcification location is given only 117 mammogram images out of 322 mammogram images.

5.1 Comparative analysis

The proposed RST based relative dependency measure algorithm is compared with the methods given in Table 4. Wu et al. [7], used a region-ranking system segmentation approach and obtaining 80% of images get accurate segmentation of mass. Dubey et al.,(2010)[5] used marker controlled watershed methods, in this work 17 mammogram images were tested for segmentation of tumor. The proposed method results are comparable with aforesaid algorithms. In the proposed work there are 117 mammogram images were used for the deduction microcalcification and segmentation. Out of the 117 mammograms, 96 images identifies and segment microcalcification in accurate position according to the radiologist specified data given in MIAS database.

Table 4. Segmentation results

Methods	Author reference	#Images used for experiment	#Acceptable (%)	#Unacceptable (%)
A region-ranking system	Wu et al. (2008)[7]	57	46(80%)	11(20%)
marker controlled watershed methods	Dubey et al(2010)[5]	17	17(100%)	0(0%)
Rough set based relative dependency measure	**Proposed**	**117**	**96(82%)**	**21(18%)**

7. Conclusion

The proposed RST based relative dependency measure algorithm for detection microcalcification and segmentation is presented. Segment the microcalcification successfully without losing any information from the rest of the mammogram. Further, the resultant mammogram can be used for the feature extraction, classification of abnormalities in human breast like calcification, circumscribed masses, spiculated masses and other ill-defined masses, circumscribed lesions, asymmetry analysis etc. This algorithm has the potential for further development because of its simplicity and it also encourages results that will motivate real-time breast cancer diagnosis system. Further, the authors are working as the classification of mammogram image using RST.

Acknowledgements

The first author immensely thanks the *UGC, New Delhi* for financial assistance under research project grant No. F.3-50/2011 (SAP-II).

The second author wholeheartedly thanks the help rendered by the UGC, SERO, Hyderabad and Aditanar College of Arts and Science, Tiruchendur to carry out this research under FDP during XI plan period.

References

[1] Breast Cancer Facts Figures, 2009–2010, American Cancer Society, Inc.

[2] J. Norum, Breast cancer screening by mammography in Norway. Is it cost-effective? (1999) 197–203.

[3] R. Ferrari, R. Rangayyan, R. Borges, A. Frere, Segmentation of the fibro-glandular disc in mammogrms using Gaussian mixture modelling, Medical and Biological Engineering and Computing 42 (3) (2004) 378–387.

[4] Arnau Oliver, JordiFreixenet, Joan Marti, Elsa Perez, Josep Pont, Erika R.E. Denton, ReyerZwiggelaar A review of automatic mass detection and segmentation in mammographic images, Medical Image Analysis 14 (2010), 87–110.

[5] R.B. Dubey, M. Hanmandlu, S.K. Gupta "A comparison of two methods for the segmentation of masses in the digital Mammograms Computerized Medical Imaging and Graphics" 34 (2010), 185–191.

[6] Alfonso Rojas Domınguez , Asoke K. Nandi Detection of masses in mammograms via statistically based enhancement, multilevel-thresholding segmentation, and region selection; Computerized Medical Imaging and Graphics 32 (2008), 304–315.

[7] Yi-TaWu, FrankY. Shih, Jiazheng Shi, Yih-TyngWu, Atop-down region dividing approach for image segmentation, Pattern Recognition 41 (2008), 1948 – 1960.

[8] K.Thangavel, M.Karnan, CAD System for Preprocessing and Enhancement Of Digital Mammograms, GVIP Journal, Volume 5, Issue 9, Dec. 2005, 69-74.

[9] Pawlak, Z.(1991) 'Rough Sets: Theoretical aspects of reasoning about data', *Kluwer Academic Publishers, Dordrecht*.

[10] Pawlak, Z.(1997) 'Rough set approach to knowledge-based decision support', *European Journal of Operational Research* Vol. 99, pp. 48-57.

[11] Skowron, A., Pawlak, Z., Komorowski, J. and Polkowski, L.(2002) 'A rough set perspective on data and knowledge'. *Handbook of data mining and knowledge discovery, Oxford University Press*, pp.134-149.

[12] Wygralak, M.(1989) 'Rough sets and fuzzy sets – some remarks on interrelations', *Fuzzy Sets and Systems*, Vol. 29(2), pp. 241-243.

[13] Gulsrud, T.O. (2000) 'Texture analysis of Digital Mammograms', *Ph.D. Thesis, Aalborg University, Stavanger, USA*, pp. 30-32.

[14] Haralick, R.M., Shanmugan, K., and Dinstein, I.(1973) 'Textural features for image classification', *IEEE Trans. Syst., Man, Cybern.*, Vol. 3(6), pp: 610–621.

[15] Haralick, R.M. (1979) 'Statistical and Structural Approaches to Texture', Proc 4th Int. Joint Conf. Pattern Recog., pp. 45-60.

[16] Velayutham, C. and Thangavel, K. "Unsupervised Feature Selection Using Rough Set", Proceedings of the International Conference on Emerging Trends in Computing (ICETC 2011), Coimbatore, 17th March 2011, pp 307-315.

[17] Velayutham, C. and Thangavel, K. "Rough Set Based Unsupervised Feature Selection Using Relative Dependency Measures", Digital Proceedings of UGC Sponsored National Conference on Emerging Computing Paradigms(2011), Dindigul, 25th Feb 2011., pp 22-36.

[18] Velayutham, C. and Thangavel, K. "Improved Rough Set Algorithms for Optimal Attribute Reduct", Journal of Electronic Science and Technology (JEST)(International), Vol. 9, No. 2, June 2011., pp 108-117.

[19] Velayutham, C. and Thangavel, K. "Unsupervised Quick Reduct Algorithm Using Rough Set Theory", Journal of Electronic Science and Technology (JEST)(International), Vol. 9, No. 3, Sep. 2011., pp 193-201.

[20] Velayutham, C. and Thangavel, K. (2012) "Unsupervised entropy based Feature Selection in digital mammogram image using rough set theory", Int. J. Computational Biology and Drug Design, Vol. 5, No. 1, pp.16–34.

[21] http://www.wiau.man.ac.uk/services/MIAS/MIASweb.html.